

## INFLUENCE OF DIFFUSION AND WETTING ON THE SiC REINFORCEMENT OF THE CAST SURFACE OF LOW ALLOY STEEL

Mohamed K. El Fawkhry and T. Mattar  
Steel Technology Department, CMRDI, Cairo, Egypt

Copyright © 2017 American Foundry Society  
DOI 10.1007/s40962-017-0151-x

### Abstract

*Reinforcement of a cast surface using a hard refractory material was used to obtain the desirable combination of toughness and wear resistance on the cast surface of a low alloy steel. Silicon carbide was chosen for its hardness and cost-effectiveness to reinforce the casting surface. The parameters that affect its interaction with the molten steel are still an issue of debate. The surface properties of the molten steel and the activity of silicon carbide have been proposed as the effective parameters in controlling the interaction between the molten steel and the solid silicon carbide. This research aims to define the role of each parameter on the SiC reinforcement of the casting surface. These two parameters were studied together and separately to identify the effect of each parameter on the depth of the*

*composite layer, the constituent phases of microstructure and the wear adhesion resistance. It was found that the dissolved oxygen in the molten steel significantly affected the depth of the composite structure layer. The addition of chromium had a great effect in producing a crack-free interface structure. The low oxygen content of steel in combination with the high percentage of active element at the composite structure increased the wear resistance of the surface of the low alloy steel (AISI1020) tenfold.*

**Keywords:** casting surface, composite structure, reinforcement of casting surface, low alloy steel cast, AISI1020, chromium addition

### Introduction

Wear-resistant cast parts are commonly produced in high alloy steel, containing a hard phase structure. Thereby, the martensitic structure in steel is considered desirable in wear condition environments.<sup>1</sup> Chromium- and molybdenum-containing steels or chromyl alloy steels usually contain a martensite structure and have been well reputed in manufacturing of such spare parts which are prone to surface wear conditions under severe duty requirements. The hard martensite phase associates with the carbide phase as a secondary phase that can strengthen the steel to withstand severe wear applications. Repeatedly, the hardness of the material was opposite to its toughness. This provides as a cornerstone in developing steel alloys to be used in surface wear conditions with sufficient endurance. Almost all the development trials have failed due to the inverse relationship between the hardness and toughness. Thereby, the development has taken a different path by developing the wear conditions of the surface while preserving the toughness of the core of material. Carburizing and/or carbonitriding have been used for this purpose, on solid steel.<sup>2</sup>

But, these methods are not applicable to cast products from an economic standpoint.

Recently, laser technology has been developed to reinforce the metal surface using a cladding technique, but it cannot also be applied on the casting surface, due to its high cost. Thus, the reinforcement of the steel casting surface must meet the quality requirements along with low process costs to be practical for casting. From this point of view, much research has been done on in situ reinforcement of the casting surface using different ferroalloys (e.g., ferrotitanium, ferrochrome, and ferrovanadium) in combination with a source of carbon to form hard refractory materials like titanium carbide, chromium carbide and vanadium carbide. The reaction between these materials has been established, utilizing the latent heat from the molten metal through solidification at the metal surface.<sup>3,4</sup> Metallurgical silicon carbide has also been suggested (for its economic advantage) in the reinforcement of the casting surface during solidification of the molten metal. Nevertheless, the nature of the interaction between the silicon carbide and the molten steel is still ambiguous. The wettability theory

in terms of wetting angle has been proposed to explain the interaction of the molten steel with the silicon carbide using Eqn. 1.<sup>5</sup>

$$\cos\theta = \sigma_{SV} - \sigma_{SL}/\sigma_{LV} \quad \text{Eqn. 1}$$

where  $\theta$  = contact angle between solid substrate and molten metal,  $\sigma_{SV}$  = surface energy between solid substrate and air,  $\sigma_{SL}$  = surface energy between solid substrate and molten metal,  $\sigma_{LV}$  = surface energy between molten metal and air.

From this perspective, the surface properties of the molten steel have a powerful effect on the interaction process based on wetting angle. In the meantime, the dissolved oxygen content of the molten steel has a great effect on the surface properties of the molten steel, especially, surface tension. On the other hand, it has been proven that the reaction of silicon carbide at the surface of the molten steel is dependent on the decomposition of silicon carbide into the molten iron. It was well proven that the presence of an active element in combination with silicon carbide can promote its decomposition into the molten iron.<sup>6</sup> The main criterion for selecting chromium as an active element was its ability to form silicides and carbides with lower Gibbs free energy than silicon carbide. Thereby, this research has been designed to contrast between the two different views to identify the most applicable method to obtain the optimum interaction between silicon carbide at the surface of the molten metal. AISI 1020 steel was selected as the molten metal in this study, due to its high toughness and its low wear resistance.

## Experimental Method

Four heats were designed by melting low-carbon steel scrap in an induction furnace with a magnesia spinel crucible. The molten metal was adjusted using ferroalloys to attain the chemical composition of AISI 1020. One heat was used as a reference for AISI 1020 steel. However, the oxygen content was changed through the other three heats using pure aluminum metal as a deoxidizer. Thereafter, the dissolved oxygen was determined as given in Eqn. 2.

$$\begin{aligned} \text{Al}_2\text{O}_3(\text{s}) &= 2[\text{Al}] + 3[\text{O}], \\ \text{K} &= [\% \text{Al}]^2 [\text{ppm}(\text{O}) * f_{\text{O}}]^3 / a_{\text{Al}_2\text{O}_3}, \\ \log \text{K} &= -62680/T + 31.85 \end{aligned} \quad \text{Eqn. 2}$$

where  $f_{\text{O}}$  = activity coefficient of oxygen dissolved in the molten metal,  $a_{\text{Al}_2\text{O}_3}$  = alumina activity with respect to the pure solid alumina,  $T$  = temperature of the molten metal (Kelvin). From this equation, the dissolved oxygen (ppm) in the molten metal can be calculated according to the aluminum content at a specific temperature. The molten metal was poured at 1600 °C, and its oxygen content ranged from 15 to 2 ppm according to aluminum content. On the other hand, nine molds were prepared using resin sand and the cavity was coated with metallurgical silicon

carbide (100–200 μm) 1% of the cavity's weight + different weight percentage of extra low-carbon ferrochrome powder (500 μm) relative to the weight of silicon carbide. Ferrochrome ranged from 0 to 1% of the silicon carbide weight. The coating was applied using a binder with an alcohol base to volatilize during mold heating at 250 °C before casting as shown in Figure 1. Table 1 shows the chemical composition of steel and Table 2 shows the fluctuation of oxygen content and chromium through the nine molds. The molds were designated with different symbols (A, B, C) according to the percentage of chromium, and accompanied by number from 0 to 2 pertaining to the level of deoxidation.

A differential scanning calorimetric (DSC) test of silicon carbide was performed by supplying 0.1 gm of silicon carbide to the meter; heating to 1500 °C at a rate of 5 °C/min in a vacuum chamber. This test determined the enthalpy change temperature. This temperature can guide to the expected chemical or physical change of silicon carbide. The reinforcement steel specimens were cut to exact dimension, were ground and polished for optical microscope observations, using a low-magnification microscope and backscattered electron (BSE) technique to observe the deep of reinforcement composite into the steel surface. High-magnification optical microscope was also used to observe the fluctuation in the structure throughout the sample from surface to core. In addition, the coherence between the composite and the main matrix was evaluated using scanning electron microscopy (SEM). Thin-layer X-ray diffraction (XRD) scanning using a Cu-source X-ray was used on the specimens after casting to identify the change in phase constituents with varying reinforcement conditions. A microhardness test was conducted to detect

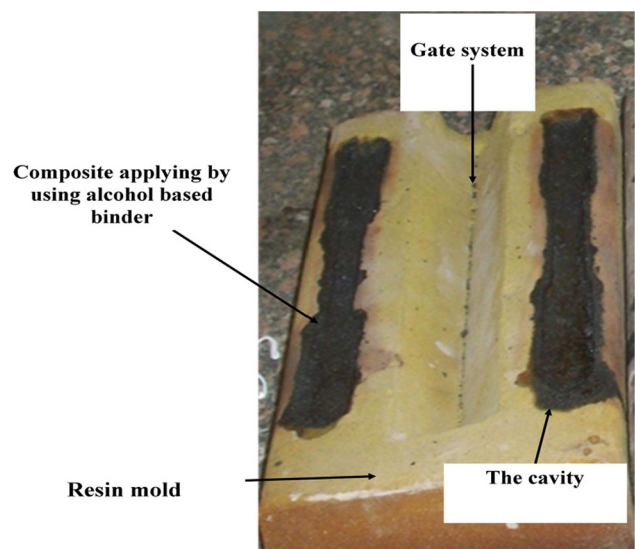


**Figure 1. Molds after coating their cavities with composite by alcoholic base binder, and after preheating at 250 °C.**

**Table 1. Chemical Composition of the Steel**

Steel grade	Chemical composition (%)					
	C	Mn	Si	S	P	Al
AISI 1020	0.14	0.45	0.12	0.048	0.035	0.047

**Table 2. Composite Structure and the Oxygen Content of the Molten Steel**

Symbol of specimens	Al%	Calculated oxygen (ppm)	Composite structure
A0	0	15	SiC + 1% Cr
A1	0.022	7.5	SiC + 1% Cr
A2	0.045	2	SiC + 1% Cr
B0	0	15	SiC + 0.5% Cr
B1	0.022	7.5	SiC + 0.5% Cr
B2	0.045	2	SiC + 0.5% Cr
C0	0	15	SiC
C1	0.022	7.5	SiC
C2	0.045	2	SiC

Cr symbol considers as an extra low carbon ferrochrome, it ranges from 0% of the weight of SiC to 1% of the weight of SiC. At zero% of chromium, Cr is not listed

the hardness of the reinforced layer with respect to the hardness of AISI1020, which was measured as 185Hv.

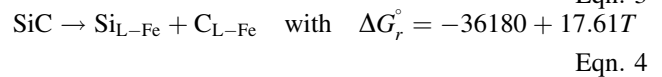
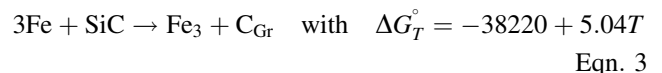
The pin on disk wear test technique was used for the ten specimens using a load of 175 N and a speed of 250 rpm. The pin specimen was 6 mm diameter, 10 mm length, and the disk was stainless steel with a diameter of 100 mm. A friction coefficient sensor was attached to the wear tester to measure the change in friction coefficient throughout the

test. Thereafter, the worn surface of the specimens was observed by using SEM.

## Results and Discussion

### Thermal Analysis of Silicon Carbide

As shown in Figure 2, DSC of silicon carbide illustrates that a significant change in its thermal character at 1200 °C may be attributed to the thermal dissociation. This means that silicon carbide will dissociate at the surface of the casting. In fact, this observation is not coinciding with the assumed results that were obtained by Cikara et al.<sup>7</sup>. Despite the thermal stability of silicon carbide, it was found that it can decompose at temperatures below 1200 °C when it is in contact with iron. Research proved that silicon carbide can be dissolved in the liquid iron to form FeSi and carbides or graphite as given in Eqns. 3, 4.<sup>8,9</sup> Thereby, it is predicted that the pearlite phase, as well as the carbide phase, might have been enriched as a result of reinforcement of the molten casting surface by silicon carbide at the expense of silicon carbide substrate.



### Macrostructure Observation

The deep etching technique was applied using Nital 3%, and the output images at low magnification were processed using AutoCAD software. By this process, it was possible to identify the depth of composite reinforcement layer on the surface of different steel specimens. Obviously, it is noticed that the oxygen content in the molten steel has a

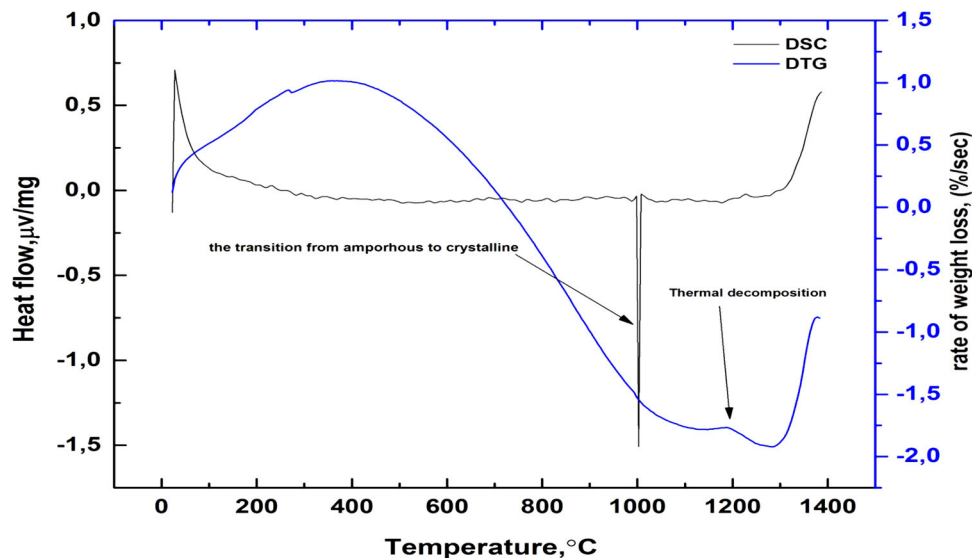


**Figure 2. DSC and DTG of silicon carbide in the range of molten metal temperature.**

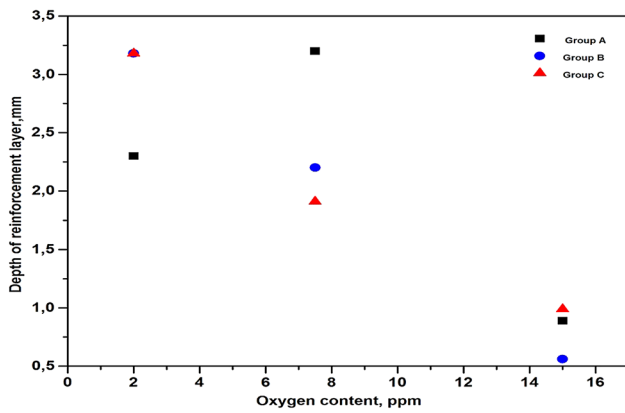


**Figure 3. Relationship between the depth of the reinforcement layer and the dissolved oxygen in the molten steel.**

significant effect on the depth of the composite on the steel surface as shown in Figures 3, 4. Concurrently, BSE images confirm the aforementioned result as shown in Figure 5. Hence, an inverse relationship between the dissolved oxygen in the steel and the wettability character of the molten steel has been confirmed, as being observed by OGINO et al.<sup>10</sup> In other words, by increasing the oxygen content in the molten steel, the wetting angle increases, and consequently the wettability of molten steel to the solid composite decreases. This fact must have affected the reactivity depth between the molten surface and the composite structure.

## Microstructure Observation

Presumably, the phase constituents will be changed in the reinforcement steel surface in the direction of the metal matrix. Microstructure observations were performed on the main three regions (surface, interface, metal matrix). Pearlite was enriched and became the main constituent phase on the surface of all reinforced steel regardless of the oxygen content as shown in Figure 6. In contrast, ferrite as the dominant phase with a bit fraction of pearlite was observed in the reference steel AISI 1020. It is clear now that the silicon carbide has thermally dissociated at the temperature of casting, which agrees with the output results from the DSC investigation of silicon carbide, and the previous studies.<sup>8,9</sup>

## Interface Layer

The interface layer between the reinforced surface structure and the main matrix structure is considered as a strong clue on the reinforcement efficiency of the casting surface by the composite. A crack-free structure in the interface layer means that a strong metallurgical bond occurred between the composite at the surface structure and the main metal matrix. The increment of the percentage of active element (chromium) in combination with silicon carbide has a positive effect in improving the interface layer between the surface structure and the main matrix as given in Figure 7. So far as the percentage of the active element in the

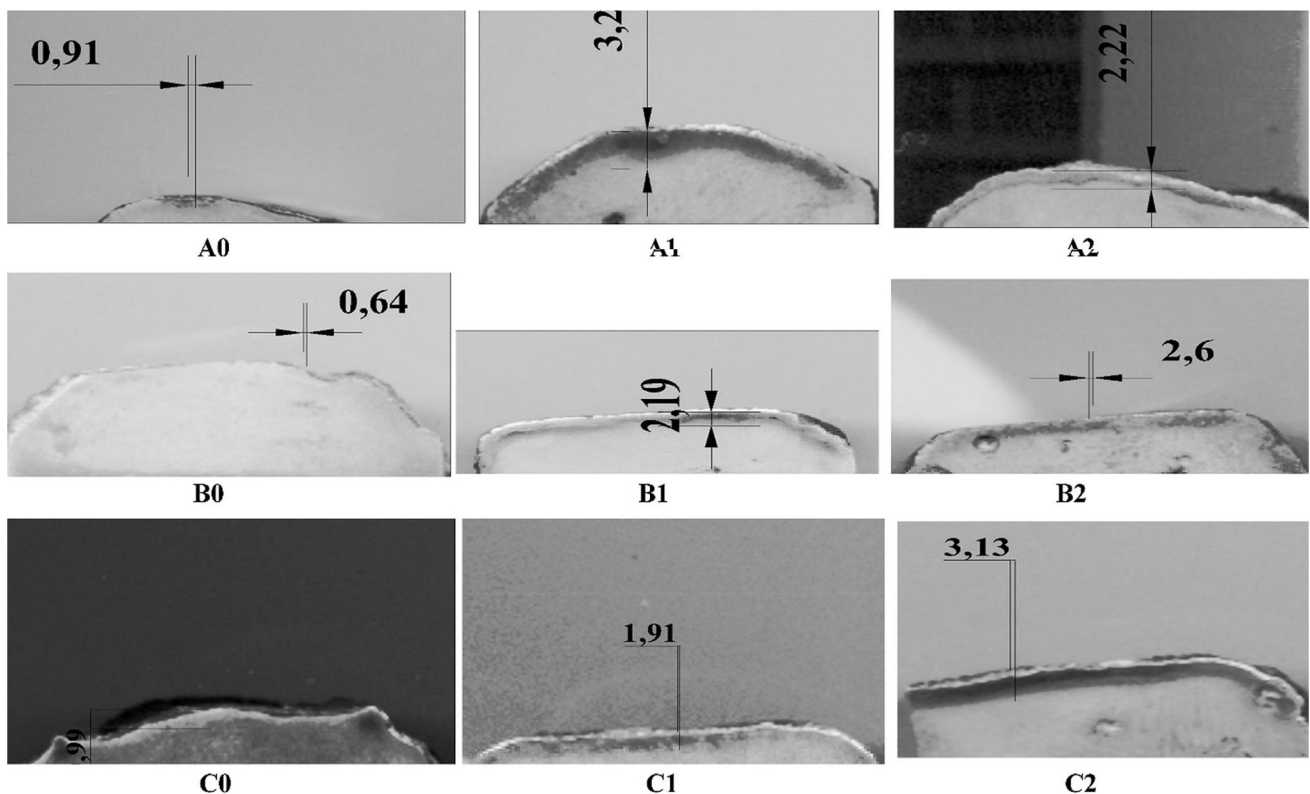


**Figure 4. Macrostructure of the specimens after casting in the different molds.**

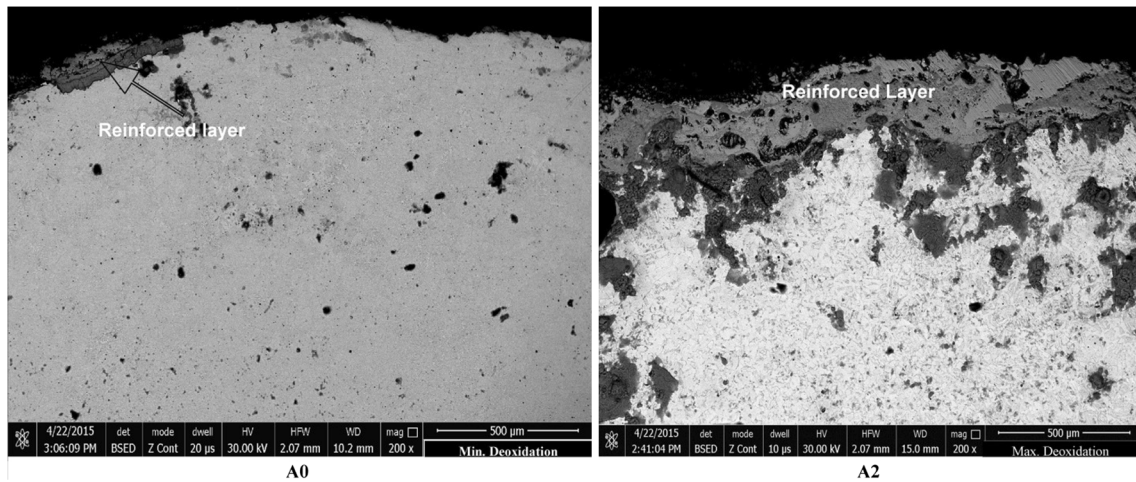


**Figure 5. Macrostructure of reinforced steel surface containing high oxygen content and low oxygen content by backscattered electron microscope.**

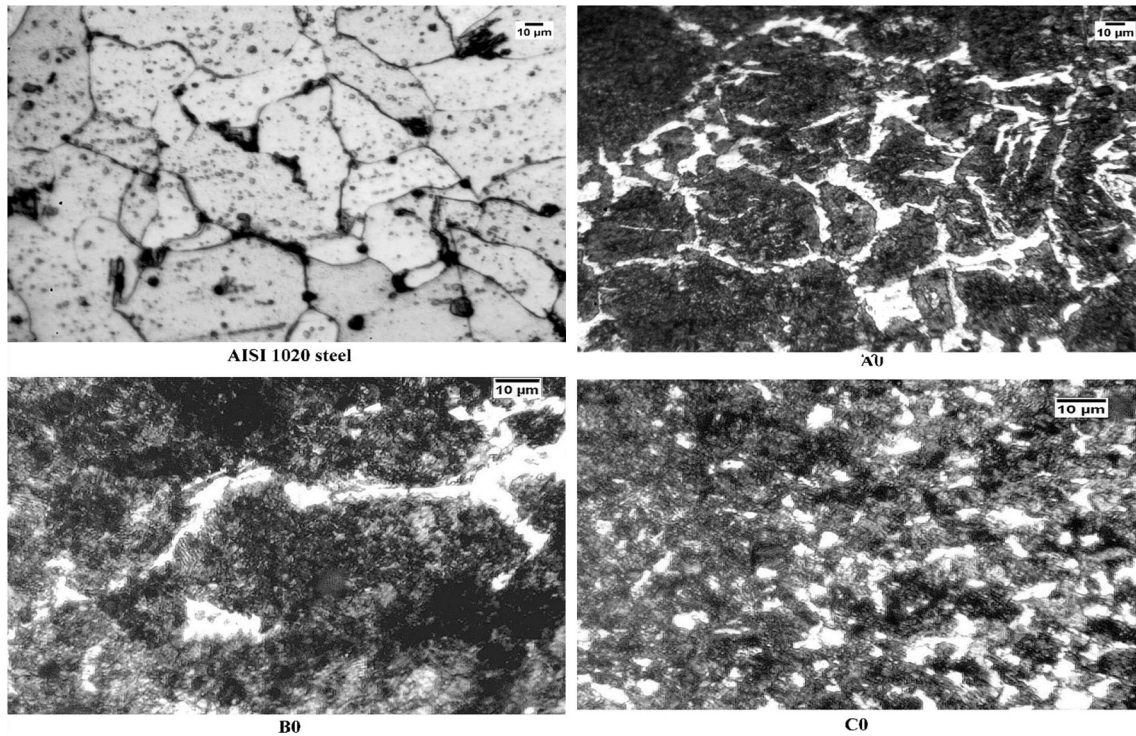
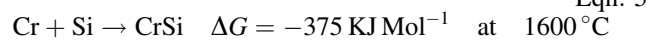


**Figure 6. Microstructure of the reinforced surface of steel of high oxygen content with different chromium content.**

composite structure is increased, the diffusion of silicon carbide into the metal matrix increases. This may be attributed to the formation of more stable silicide and carbide through the reaction of SiC with the active element (chromium) as given in Eqns. 5, 6.<sup>11</sup> On the other hand, it was found that the microcrack between the interface layer and the matrix metal can be observed at low oxygen content of the molten metal as given in Figure 8. This proved that the dissolved oxygen in the molten steel has a negligible role on the nature of the interface layer.



Eqn. 5



Eqn. 6

### XRD Observation

XRD analysis was applied using thin-layer scanning methodology, in which the scanning of the X-ray was

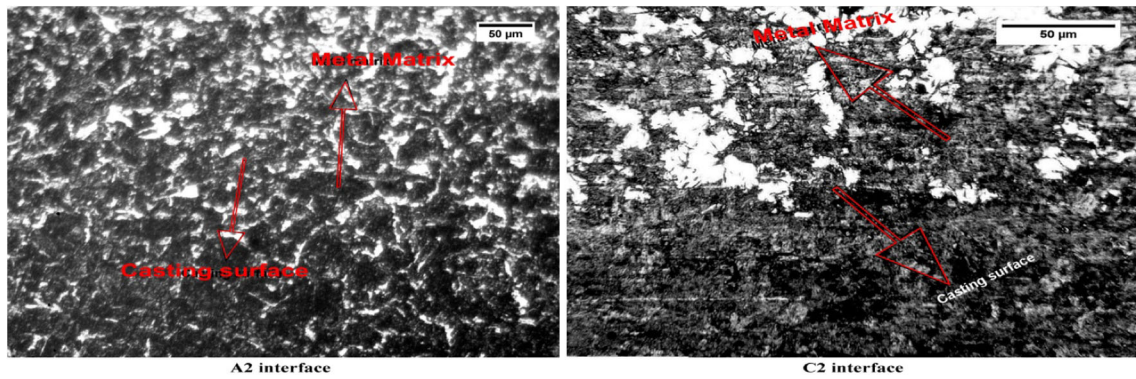


**Figure 7.** Optical microstructure observation of the interface layer of surface reinforced by high percentage of active element and low percentage of active element.

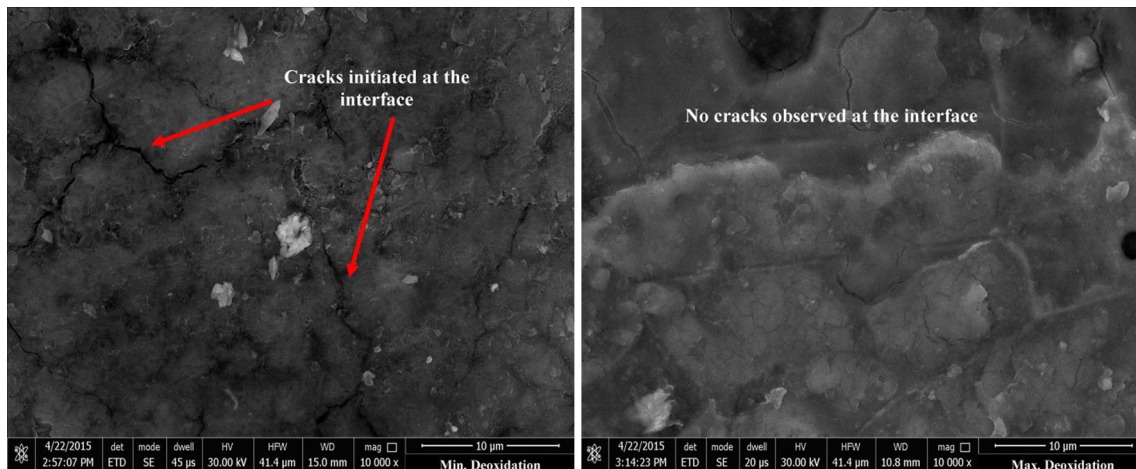


**Figure 8.** Microcracks observation by SEM in the interface layer of low- and high-oxygen-containing reinforced steel.

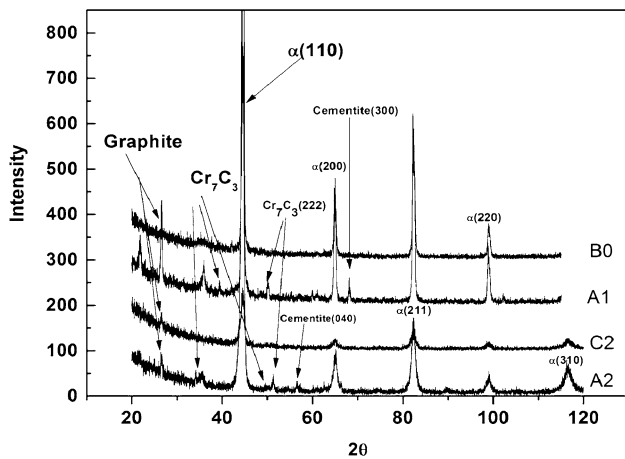


**Figure 9.** Thin-layer XRD of different reinforced steels.

performed on 5 mm thickness of the specimen from the reinforced surface. XRD analysis coincides to the obtained microstructure observations as shown in Figure 9. Chromium carbide  $Cr_7C_3$  is formed in the steel reinforced by the combination of silicon carbide and chromium, due to its low Gibbs free energy. However, chromium silicide has

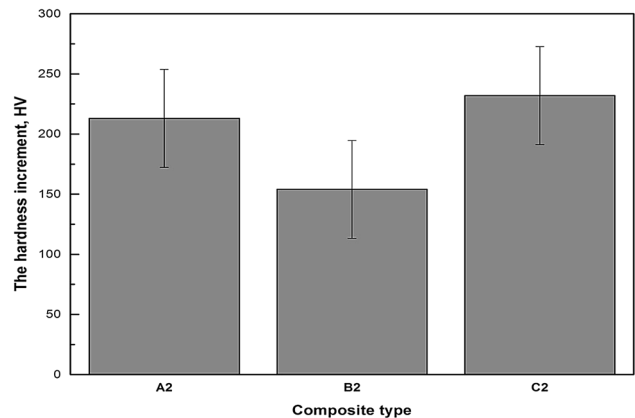


**Figure 10.** Hardness increment through the steel reinforced by different composite structure.

never been observed in the same conditions. In the meantime, graphite has been observed in the steel reinforced with silicon carbide mixed with a high percentage of chromium (A group). This can be explained by the affinity of chromium to form  $Cr_7C_3$  at the expense of chromium silicide, resulting in enrichment of silicon in the matrix

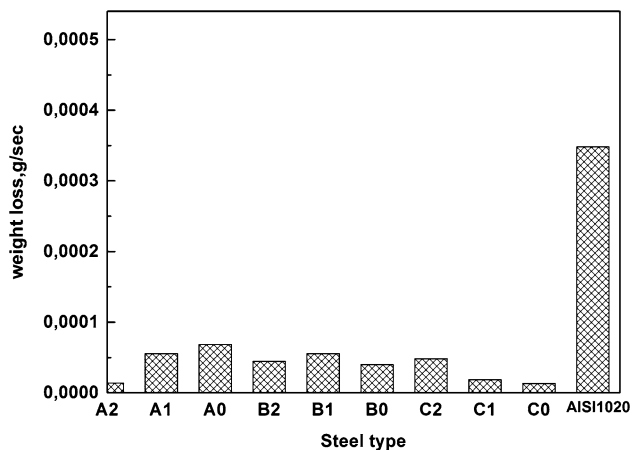


Figure 11. Weight loss of the wear-tested steels.

which promotes the graphite precipitation. No significant peaks were observed for the silicon carbide, which assures its decomposition during the casting temperature as described later by Eqns. 3, 4.

### Hardness Investigation

The hardness increment was studied by HV30 hardness test at the reinforced surface, and the values were compared with the hardness of AISI 1020 steel that was basically found to be 185 HV. It is well known that the secondary

phase formed as a result of reinforcement must have the main powerful effect on the enhancement of hardness value.<sup>12</sup> Cementite and chromium carbides are considered as the main secondary phases that are enriched at the surface as a result of composite reinforcement. The hardness increment in the steel surface with low oxygen content reinforced by silicon carbide (C2) is much higher than those were reinforced by silicon carbide and chromium (A2) as shown in Figure 10. No doubt, cementite has a high hardness value (>600HV) and is largely formed on the steel surface reinforced by silicon carbide without active element as given in XRD chart. Hardness is one of the factors that affect the surface wear resistance, but it will not be the key player in the wear resistance property as will be discussed later.

### Wear Adhesion Behavior

The reinforcement of the casting surface is mainly aimed at improving the surface performance against wear conditions. Thereby, the wear test of the reference steel and the other nine steels were carried out by using pin on disk technique at a speed of 250 rpm, and load 175 N for 17 min to obtain the appropriate results, simulating the real state. The values of the weight loss of the wear-tested steels indicated much improvement in the wear resistance character of the reinforced steel surface by different percentage of composite structure in comparison with the weight loss

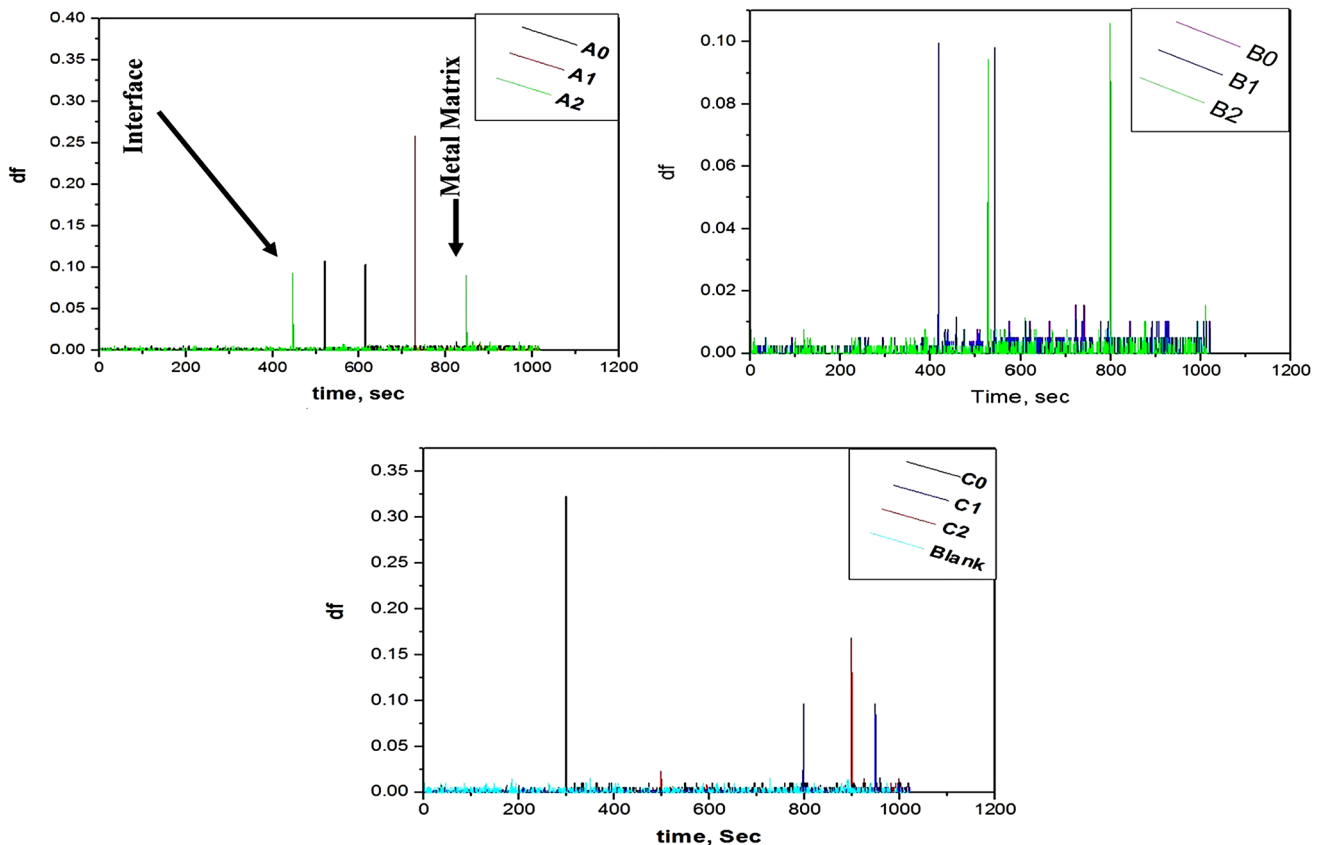
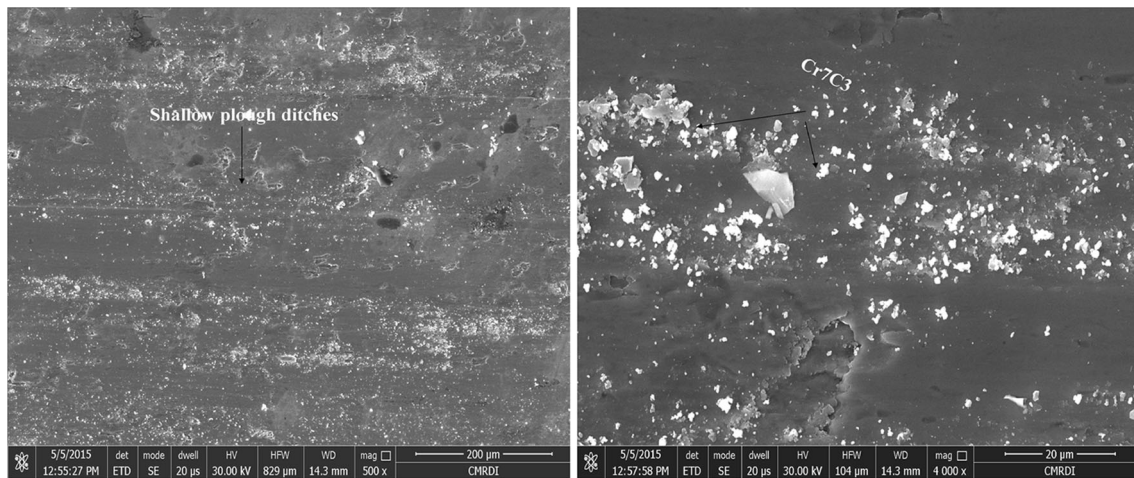


Figure 12. First derivative of the wear friction coefficient of the steel after composite reinforcement.



**Figure 13. SEM of the worn surface of steel A2.**

of the reference steel AISI 1020. The variation in the weight loss through the ten tested steels gives us an ambiguous image on the effect of reinforcement process on the metal surface by using different conditions. However, the most significant improvement was observed at the low-oxygen-containing steel that was reinforced by a combination of silicon carbide with high chromium content (A2) as shown in Figure 11. Thereby, the first derivative of friction coefficient was calculated to find out the behavior of the material through the wear test as given in Figure 12. It was observed that the transition change either at the interface layer or at the main matrix layer is significant in steel surface reinforced by silicon carbide (C group) or reinforced by silicon carbide + 1% chromium (A group). Certainly, the power of change explains the large dissimilarity through the three phases (composite, interface, and main matrix). In addition, it can be observed that the depth of the interface layer is inversely proportional to the oxygen content in the molten steel, which was proved already in the macrostructure observations.

### Worn Surface by SEM

The worn surface of the wear specimens was observed using a high-magnification electron microscope to track the wear mechanism at the surface of reinforced steels. Shallow plow ditches were observed on the worn surface of the low-oxygen-containing steel reinforced by silicon carbide and 1% of chromium (A2) as shown in Figure 13. EDS analysis of the precipitates that have been observed in the wear route reveal the powerful role of chromium carbide  $\text{Cr}_7\text{C}_3$  against the wear mechanism.<sup>13</sup>

### Conclusion

The oxygen content in the molten metal reduces the wettability of the molten metal to a solid substrate, and consequently delays the interaction between the solid substrate

and the molten metal. In fact, this has a great effect on the reinforcement depth of the casting surface by silicon carbide. However, using an active metal with silicon carbide in the reinforcement technology has a positive impact in forming good metallurgical bonding between the metal matrix and the reinforcement surface layer. XRD analysis refers to the possibility of graphite precipitation in the microscale at the reinforcement surface layer of the low-oxygen-containing steel, owing to the silicon enrichment in the metal matrix. Hardness increment has been observed in the reinforced surface layer either by using SiC or SiC + Cr. The increment of hardness has positively reflected on their wear resistance compared with the reference steel AISI 1020. In addition, SEM in conjunction with EDS analysis of the worn surface assures the powerful effect of  $\text{Cr}_7\text{C}_3$  precipitates on the progress of the wear mechanism.

### REFERENCES

1. J. Kalousek, D.M. Fegredo, E.E. Laufer, The wear resistance and worn metallography of pearlite, bainite and tempered martensite rail steel microstructures of high hardness. *Wear* **105**(3), 199–222 (1985)
2. R. Collin, S. Gunnarson, D. Thulin, Influence of reaction rate on gas carburizing of steel in a  $\text{CO-H}_2\text{-CO}_2\text{-H}_2\text{O-CH}_4\text{-N}_2$  atmosphere. *J. Iron Steel Int.* **210**(10), 777–784 (1972)
3. Y. Wang, X. Zhang, G. Zeng, F. Li, In situ production of Fe-VC and Fe-TiC surface composites by cast-sintering. *Compo. Part A Appl. Sci. Manuf.* **32**(2), 281–286 (2001)
4. C. Cui, Z. Guo, H. Wang, J. Hu, In situ TiC particles reinforced grey cast iron composite fabricated by laser cladding of Ni-Ti-C system. *J. Mater. Process. Technol.* **183**(2), 380–385 (2007)



5. J.P. Rocher, J.M. Quenisset, R. Naslain, Wetting improvement of carbon or silicon carbide by aluminium alloys based on a  $K_2ZrF_6$  surface treatment: application to composite material casting. *J. Mater. Sci.* **24**(8), 2697–2703 (1989)
6. G.W. Liu et al., Survey on wetting of SiC by molten metals. *Ceram. Int.* **36**(4), 1177–1188 (2010)
7. D. Čikara, M. Rakin, A. Todić, Cast Steel-SiC composites as wear resistant materials. *FME Trans.* **37**(3), 151–155 (2009)
8. T.C. Chou, A. Joshi, Selectivity of silicon carbide/stainless steel solid-state reactions and discontinuous decomposition of silicon carbide. *J. Am. Ceram. Soc.* **74**(6), 1364–1372 (1991)
9. J. Li, H. Ru, H. Yang, Y. Liu, Liquid–Solid reactions and microstructure of SiC-5120 steel composite brake material. *Metall. Mater. Trans. A* **43**(2), 658–664 (2012)
10. K. Ogino, K. Nogi, O. Yamase, Effects of selenium and tellurium on the surface tension of molten iron and the wettability of alumina by molten iron. *Trans. Iron Steel Inst. Jpn.* **23**(3), 234–239 (1983)
11. J.S. Park, K. Landry, J.H. Perepezko, Kinetic control of silicon carbide/metal reactions. *Mater. Sci. Eng., A* **259**(2), 279–286 (1999)
12. M.F. Buchely et al., The effect of microstructure on abrasive wear of hard facing alloys. *Wear* **259**(1), 52–61 (2005)
13. G.F. Sun, Y.K. Zhang, C.S. Liu, K.Y. Luo, X.Q. Tao, P. Li, Microstructure and wear resistance enhancement of cast steel rolls by laser surface alloying NiCr–Cr<sub>3</sub>C<sub>2</sub>. *Mater. Des.* **31**(6), 2737–2744 (2010)